Energy Redistribution due to the Cloud Layer - Preliminary Results for Shortwave Cloudy Closure

P. Wang, W. H. Knap

Royal Netherlands Meteorological Institute (KNMI),
P.O. Box 201, 3730 AE De Bilt, The Netherlands, Email: wangp@knmi.nl

ABSTRACT

Radiation is the ultimate source and sink for the climate system. Due to the presence of clouds, radiative energy is vertically redistributed. The shortwave irradiance at the surface generally decreases during overcast conditions. However, at the top of atmosphere the irradiance increases because of the high reflectance of clouds. To consider the energy redistribution inside the cloud layer and above/ below the cloud we used the radiative transfer model DAK (Doubling Adding KNMI) to calculate heating rates and flux profiles for overcast cases. Atmospheric profiles were derived by means of the Integrated Profiling Technique (IPT). Simulated irradiances at the surface are compared with ground-based BSRN measurements.

1. INTRODUCTION

Aerosol and cloud radiative forcing have been intensively studied world wide using both observations and models. Satellite-based radiation budgets in combination with radiative transfer model calculations and other observations have provided us with a rough conceptual understanding of the distribution of cloud-induced heating within the atmosphere and at the surface [1, 2, 3]. Recently, Mace et al, [4, 5] have studied the redistribution of heat in the atmosphere by clouds using measurements and models at SGP/ARM (Southern Great Plains / Atmospheric Radiation Measurement) site. McFarlane et al. [6] studied the effect of clouds on the calculated vertical distribution of shortwave absorption in the tropics using data at Nauru and Manus at the TWP/ARM (Tropical Western Pacific) site.

In the Netherlands, the CESAR Observatory (Cabauw Experimental Site for Atmospheric Reseach) consists of a large set of instruments to study the atmosphere and its interaction with the land surface. The site is used for monitoring of long term tendencies in atmospheric changes, studies of atmospheric and land surface processes for climate modeling, validation of space-borne observations, the development and implementation of new measurement techniques (http://www.cesar-observatory.nl). Loehnert et al., [7, 8] have developed the Integrated Profiling Technique (IPT) algorithm to derive physically consistent profiles of temperature, humidity and cloud liquid water content using combined radar, lidar, microwave radiometer and synoptic observations. Now the IPT algorithm runs operationally for Cabauw. Since 2005, the radiation site of Cabauw has been part of the Baseline Surface Radiation Network (BSRN) [9, 10].

In May 2008 the EUCAARI-IMPACT campaign was executed at Cabauw. During this campaign excellent shortwave broadband irradiance closure has been achieved on the basis of AERONET and BSRN measurements for clear sky cases [11]. The good results are not only the result of high-quality measurements but also of intense development of the DAK radiative transfer model. Ongoing work at KNMI consists of shortwave closure at the surface for overcast cases and the radiation profile for cloudy cases. In this paper we will show some preliminary results about the closure study for the overcast case and explain the ideas for the radiation profiles.

2. METHODS

The flux profile and heating rate can be calculated using the Doubling Adding KMNI (DAK) radiative transfer model [12, 13, 14, 15]. We start from the shortwave radiative closure between DAK model simulations and BSRN measurements for the simple overcast case with one single layer stratocumulus water clouds. For water clouds the scattering phase matrices are calculated using Mie theory [16]. The cloud phase matrices have been calculated at 32 wavelengths and for 14 particle sizes. The broadband surface irradiances are calculated at 32 wavelength bands from 240-4600 nm using k-distribution methods for the absorption of O_2, CO_2, O_3 and water vapor [17]. However, it is still too time consuming to do online calculations for the cloudy cases. Therefore the direct, diffuse, global irradiance at surface are pre-calculated at 24 cloud optical thickness (from 0 to 160), 14 effective radii (from 2 to 20 micron) and 10 solar zenith angles (0-75°). In comparison to the effect of clouds, the effects of O_3, water vapor and aerosols on the diffuse irradiance are small, so we use the standard mid-latitude summer atmospheric profile (including O_3 and water vapor) and no aerosols. For relatively thick clouds the direct irradiance at surface is close to 0, the fixed O_3 and H_2O profile only cause a very small error in the global irradiances. In the DAK simulations we assume that the cloud is a homogenous layer at 1-2 km because the effect of cloud altitude on the irradiance at the surface can be neglected. The diffuse irradiances for SZA = 60° are shown in Fig. 1 as an example for the LUT. The diffuse irradiance at the surface decreases with increasing cloud optical thickness. The diffuse irradiance increases with increasing effective radius, however the increase is small for effective radii larger than 10.

The most important parameter for the cloudy radiative transfer is the cloud optical depth (COD) (cloud optical thickness (COT) at every altitude layer). Currently the

© Proceedings of the 8th International Symposium on Tropospheric Profiling, ISBN 978-90-6960-233-2
Delft, The Netherlands, October 2009. Editors, A. Apituley, H.W.J. Russchenberg, W.A.A. Monna

cloud liquid water content profile and effective radius (R_e) profile are available from the IPT data for water clouds at Cabauw. The microwave radiometer also provided liquid water path (LWP). The LWP, R_e and COT are also available from MODIS, SEVIRI and other satellite measurements. The cloud optical thickness can be calculated as follows:

$$COT = \frac{2LWP}{3R_e\rho} \qquad (1)$$

where ρ is the density of liquid water. The cloud optical depth can be calculated using Eq. 1 except that the LWP and R_e should be profiles instead of integrated values.

Actually it is sufficient to use cloud optical thickness for the closure studies. In this paper we also use the collocated cloud optical thickness from MODIS to check the closure at surface because this is more straightforward. If the MODIS data give better closure than the IPT data the IPT cloud optical thickness will be scaled to the MODIS optical thickness.

If closure is achieved we have confidence that the cloud optical thickness is in good shape. Therefore the cloud optical depth profile derived from the IPT profile using Eq. 1 is reliable. The radiative forcing profiles and heating rates at the 32 bands can be calculated using the DAK model with the same settings that give good closure with BSRN measurements. In an ideal case the closure should be achieved simultaneously at the top of atmosphere and at the surface.

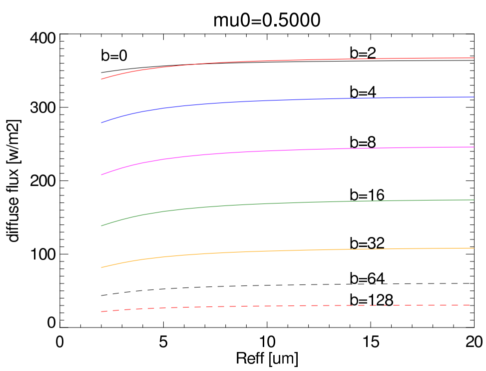

Figure 1. *Diffuse irradiance at surface as a function of effective radius for different cloud optical thicknesses at SZA of 60° for water clouds. 'b' is optical thickness.*

3. RESULTS AND DISCUSSION

The shortwave radiation closure and radiative forcing profile are our ongoing work. We could only show some very preliminary results here. An overcast case was selected from radar/lidar measurements on 30 January 2007. As shown in Fig. 2 on this day the clouds were one single layer and no ice clouds.

In this paper we used MODIS L2 cloud data at 5km spatial resolution [18]. The MODIS data were selected over Cabauw within 10-km radius. There are two times MODIS overpass per day, so we only have two measurements from MODIS to compare with IPT and microwave radiometer data. The microwave radiometer and LPT measurements have very high time resolution and are averaged in 10 minutes intervals in this study.

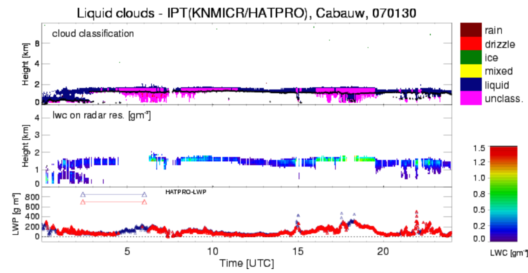

Figure 2. *Clouds classification, heights and LWP on 30 January 2007 at Cabauw.*

We had three different cloud optical thicknesses: 1) calculated from IPT integrated cloud liquid water content and R_e using Eq. 1; 2) calculated from microwave radiometer LWP and MODIS R_e using Eq. 1; 3) selected from collocated MODIS L2 data. The cloud optical thickness derived from microwave radiometer and MODIS are shown in Fig. 2.

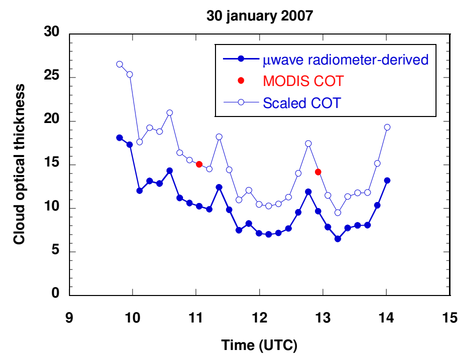

Figure 3. *Cloud optical thickness time series derived from microwave radiometer and the scaled COT to MODIS on 30 January 2007.*

On 30 January 2007 the COT derived from the microwave radiometer using averaged MODIS R_e is lower than MODIS optical thickness. The IPT LWP is lower than microwave radiometer therefore the IPT COT is also lower MODIS. Using MODIS COT the simulated diffuse irradiances at surface are comparable to BSRN measurements. Therefore we scaled the COT derived from microwave radiometer to the mean MODIS COT at 11 and 13 UTC. The scaling factor is about 1.6. Since the clouds were relative stable on that day it was reasonable to use one scaling factor for the whole day. Fig. 4 shows the global irradiances measured by BSRN and the simulated global irradiances interpolated from the LUT using the scaled COTs. The differences are within +/- 15 W/m^2. The mean difference is 5 W/m^2. The simulated global irradiances follow the variations of BSRN measurements. Between 11 and 13 UTC the simulated irradiances are higher than BSRN measurements. Between 9 and 11 UTC the simulated irradiances are lower. That might be due to the fact that the scaling factor is computed using MODIS COT close to 11 and 13 UTC. If we use the COT derived from IPT and scaled to MODIS the simulated global irradiances are also close to the BSRN measurements.

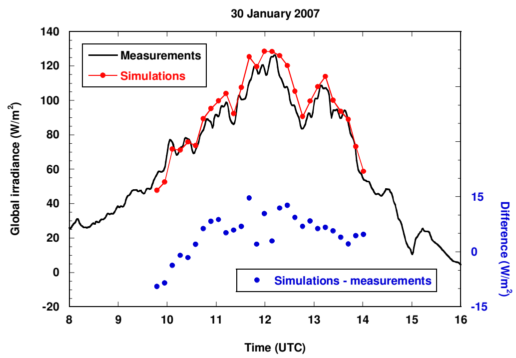

Figure 4. *Global irradiances from simulations using the scaled microwave radiometer COT and the BSRN measurements for 30 January 2007.*

The microwave radiometer and lidar/radar measurements have a narrow field of field. They are more sensitive to the inhomogeneous character of the clouds. The BSRN global irradiance is measured hemispherically and the irradiances are the average of a large area over the instruments. This could be seen from the variations of the BSRN data and ITP or microwave radiometer data. The average of 10 minutes leads to similar variation in the two data sets. However, there should be a more robust method for the temporal and spatial match.

By comparing the COT derived from IPT and microwave radiometer with MODIS we have to take into account their spatial resolution. MODIS provides a 1-km cloud product but the resolution is still very different as compared to the radar/lidar vertical beam. If the clouds are inhomogenous the COT will be different for the lidar/radar method and MODIS product. When using the derived COT for model simulations and compare these to BSRN measurements, there is another spatial resolution difference. We assumed that the BSRN instruments receive photons within 10 km for cloudy cases. This might be different for different cloud cases.

The clouds were about 300 m thick and contained relatively little water on 30 January 2007, which might not be an optimal case for the IPT algorithm. Therefore we need more cases to test our approach for the cloudy closure.

4. CONCLUSION

We have performed a one case study of shortwave radiative closure for an overcast case on 30 January 2007 at Cabauw. The simulated global irradiances using the scaled cloud optical thicknesses derived from microwave radiometer or IPT data are comparable to BSRN global irradiances. The mean difference between simulations and measurements is 5 W/m^2. The result is promising. However, the scaling will not work if the clouds have large temporal variations since only two MODIS overpasses per day are available. Without scaling the cloud optical thickness derived from IPT or microwave radiometer is relatively small, so that the simulated global irradiances are much smaller than BSRN measurements. Therefore we plan to use the cloud properties from SEVIRI/MSG, which has 15 minutes time resolution. After we get robust closure we can calculate reliable cloud radiative forcing profiles.

REFERENCES

[1] Rossow, W. B., and T.-C. Zhang, 1995: Calculation of surface and top of atmosphere radiative fluxes from physical quantities based on ISCCP data sets: 2. Validation and first results*, J. Geophys. Res.,* 100, 1167–1197.

[2] Bergman, J. W., and H. H. Hendon, 1998: Calculating monthly radiative fluxes and heating rates from monthly cloud observations, *J. Atmos. Sci.*, 55, 2471–3491.

[3] Chen, T., W. B. Rossow, and Y. Zhang, 2000: Radiative effects of cloudtype variations, *J. Clim.*, 13, 264– 286.

[4] Mace, G. G., et al., 2006: Cloud radiative forcing at the Atmospheric Radiation Measurement Program Climate Research Facility: 1. Technique, validation, and comparison to satellite-derived diagnostic quantities*, J. Geophys. Res.,* 111, D11S90, doi:10.1029/2005JD005921.

[5] Mace, G. G., S. Benson, and S. Kato, 2006: Cloud radiative forcing at the Atmospheric Radiation Measurement Program Climate Research Facility: 2. Vertical redistribution of radiant energy by clouds, *J. Geophys. Res.*, 111, D11S91, doi:10.1029/2005JD005922.

[6] McFarlane, S. A., J. H. Mather, T. P. Ackerman, and Z. Liu, 2008: Effect of clouds on the calculated vertical distribution of shortwave absorption in the tropics, *J. Geophys. Res.,* 113, D18203, doi:10.1029/2008JD009791.

[7] Loehnert, U. S. Crewell, and C. Simmer, 2004: An Integrated Approach toward Retrieving Physically Consistent Profiles of Temperature, Humidity, and Cloud Liquid Water*, J. Appl. Meteor.* vol. 43 1295-1307.

[8] Loehnert, U., E. van Meijgaard, H. K. Baltink, S. Groß, and R. Boers, 2007: Accuracy assessment of an integrated profiling technique for operationally deriving profiles of temperature, humidity, and cloud liquid water, *J. Geophys. Res.,* 112, D04205, doi:10.1029/2006JD007379.

[9] Ohmura, A et al., 1998: Baseline Surface Radiation Network (BSRN/WCRP): New Precision Radiometry for Climate Research, *Bulletin of the American Meteorological Society*, 79(10), 2115–2136, DOI: 10.1175/1520-0477(1998)079.

[10] Knap, W. H., J. Bijma, Y. B. L. Hinssen, A. Los, C. van Oort, J. Warmer, E. Worrell, 2007: The Baseline Surface Radiation Network (BSRN) station at the Cabauw Observatory. KNMI Biennial Scientific Report 2005-2006, 18-23.

[11] Wang P., W. H. Knap, P. Kuipers Munneke, P. Stammes, 2009: Clear-sky shortwave radiative closure for the Cabauw Baseline Surface Radiation Network site, Netherlands, J. Geophys. Res., 114, D14206, doi:10.1029/2009JD011978.

[12] De Haan, J.F., P.B. Bosma and J.W. Hovenier, 1987: The adding method for multiple scattering com-

putations of polarized light, *Astron. Astrophys.* 183, p. 371-391.

[13] Stammes, P., 2001: Spectral radiance modelling in the UV-Visible range, in: IRS 2000: Current problems in Atmospheric Radiation, Eds. W.L. Smith and Y.M. Timofeyev, A. Deepak Publ., Hampton, VA, 385-388.

[14] Kuipers Munneke, P., C. H. Reijmer, M. R. van den Broeke et al., 2008: Analysis of clear-sky Antarctic snow albedo using observations and radiative transfer modeling, *J. Geophys. Res.*, 113, D17118, doi:10.1029/2007JD009653

[15] Wang, P., W. H. Knap, P. Kuipers Munneke, P. Stammes, 2008: Clear-sky atmospheric radiative transfer: a model intercomparison for shortwave irradiances, accepted in International Radiation Symposium 2008 (IRS 2008) proceeding.

[16] de Rooij, W.A. and C. van der Stap, 1984: Expansion of Mie Scattering Matrices in Generalized Spherical Functions, *Astron. Astrophys.* 131, p. 237.

[17] Kato, S., T. P. Ackerman, J. H. Mather, and E. E. Clothiaux, 1999: The k-distribution method and correlated-k approximation for a shortwave radiative transfer model, *J. Quant. Spectrosc. Radiat. Transfer*, 62, 109– 121.

[18] King, Tsay, Platnick, Wang, & Liou, 1998: Cloud Retrieval Algorithms for MODIS: Optical Thickness, Effective Particle Radius, and Thermodynamic Phase. Products: MOD06, MOD08. ATBD Reference Number: ATBD-MOD-05.